Electrochemical behavior of spray deposited nickel oxide (NiO) thin film in Alkaline electrolyte

Bilal Brioual[1*], *Zaid* Rossi[1], *Abdessamad* Aouni[1], *Mustapha* Diani[1], *Mohammed* Addou[1], and *Mohammed* Jbilou[1]

[1]Equipe de recherche en Couches Minces et Nanomatériaux (CMN), FST, Université Abdelmalek Essâadi, Tanger-Maroc, Morocco

Abstract. Nickel oxide (NiO) Thin film was successfully deposited on the glass substrate using an inexpensive spray pyrolysis (SP) technique. The structural, morphological, and optical properties have been studied, thus the electrochemical behavior of NiO film in Alkaline electrolytes has been investigated. The X-ray diffraction (XRD) analysis showed that NiO thin film exhibit a polycrystalline cubic rock-salt structure with a preferential orientation on the plane (111). This result was confirmed using Raman spectroscopy. The Scanning Electron Microscopy (SEM) images exhibit a smooth and dense surface without major cracks. Optical analysis shows an average transmission of about 55% in the visible light range, and the optical band gap energy was estimated by Tauc's method and showed a value of 3,71 eV. Electrochemical properties as specific capacitance (Csp), optical density variation (ΔOD), and Coloration efficiency (CE) were studied using cyclic voltammetry in 1M KOH and 1M NaOH electrolytes. The results indicated that the behavior of the NiO layer in KOH is more effective than in NaOH electrolytes.

1. Introduction

For several years, transition metal oxides have attracted a noticeable attention of researchers due to their promising characteristics for various application fields. Among these materials, nickel oxide (NiO) is an attractive material because of its good magnetic, thermal, optical, mechanical and, electrical performance [1], [2], [3]. The stoichiometric NiO crystal is an insulator, whereas the conductivity can be enhanced in pure NiO by creating Ni vacancies [4]. The most attractive properties of NiO are; low material cost, wide bandgap semiconductor (3.6–4.0 eV) [5], excellent electrochemical stability [6], and finally the possibility of synthesis by a variety of techniques [7].

NiO layers can be used in many applications, including photo-catalysts [8], optoelectronic devices [9], antiferromagnetic layers [10], solar cells [11], gas sensors [12], supercapacitors [13], and electrochromic devices [14]. In electrochemistry, NiO thin films can be used as Counter-electrode, which WO_3 is the Work-electrode (WE) in electrochromic devices (ECDs) [15], due to its high coloration efficiency (CE), its fast switching between the decolored and colored states, its good cyclic reversibility and memory effect [16].

Various methods were used to prepare NiO thin layers, such as chemical vapor deposition (CVD) [17], atomic layer deposition (ALD) [18], dc-magnetron sputtering [19], pulsed laser deposition (PLD) [20], electron-beam evaporation [21], spray pyrolysis [22], sol-gel process [23], chemical bath deposition (CBD) [24] and the electrodeposition process etc. [1], [25]. Among these methods, the spray pyrolysis technique has many advantages; economical, easy to prepare and permits to control the deposition conditions without the need of high vacuum and offers the possibility for large area deposition [22].

In this work, a thin film of NiO was synthesized by the spray pyrolysis method. The structural, optical, and morphological properties of the NiO layer have been studied. Thus, the electrochemical behavior in Alkaline electrolytes has been demonstrated using cyclic voltammetry (CV).

2. Experimental procedure

Before depositing the film, the glass substrates were cleaned chemically in Acetone, Ethanol, and dilute hydrochloric acid (HCl) respectively for 15 minutes in each solution, separated by rinsing in distilled water. Then several tests were made to find the optimal conditions for the preparation of the specimen using the spray pyrolysis method. A detailed description of this technique has been explained in [26]. After the optimization of parameters, a NiO thin layer was deposited on an amorphous glass substrate preheated at 450°C. This temperature was

*Corresponding author: bilal.brioual@etu.uae.ac.ma

chosen during the optimization of the deposit parameters because, at other temperatures such as 350, 400 and 500, impurities have appeared in the thin films such as H_2O and metallic nickel. 0,025 mol/l of hexahydrate nickel chloride ($NiCl_2$ •$6H_2O$) was used as a precursor and dissolved in 50 ml of distilled water. The deposit parameters are summarized in Table 1.

Table1. Deposition parameters of the spray pyrolysis technique.

Parameters	Values
Precursor concentration	0,025 M
Solution flow rate	1,5 ml/ min
Compressed air pressure	0,5 bar
Spray time	8 minutes
Substrate temperature	450 °C
Nozzle-Substrate distance	40 cm

3. Characterization techniques

X-ray diffraction analysis (XRD) was performed using a D8 ADVANCE X-ray diffractometer (λKα1, Cu). To confirm the crystalline phase a micro-Raman spectroscopy SENTERRA II, with a laser source set at 532 nm was used. The SHIMADZU Ultraviolet-Visible Near Infrared (UV-Vis-NIR) spectrometer was adopted to inspect the optical properties. The morphological characteristics were explored by scanning electron microscopy (SEM), with an accelerated voltage at 10 kV, a magnification of x40K, and an emission current of 120 µA.

For the electrochemical study, NiO thin film was deposited on Indium Tin Oxide (ITO) substrate. This film was immersed in two different electrolytic solutions. The first is 1M KOH and the second is 1M NaOH. The cyclic voltammetry measurements were based on a three-contact electrode system; saturated calomel (SCE) as the reference, a platinum sheet as a back-contact electrode, and NiO/ITO as the working electrode.

4. Results and discussion

4.1. X-ray diffraction results

The XRD diagram of the NiO layer deposited on a glass substrate is shown in Figure 1. The pattern shows a polycrystalline film with a cubic structure. The diffraction peaks observed at the 2θ diffraction angles 37,26°; 43,31° and 79,36° are attributed to the crystallographic planes (111), (200) and (222), respectively with a strong preferred orientation corresponding to the direction (111). Using the International Center for Diffraction Data (ICDD) card number (04–0835), these peaks are indexed in a cubic rock-salt structure. These results match other studies [27], [28].

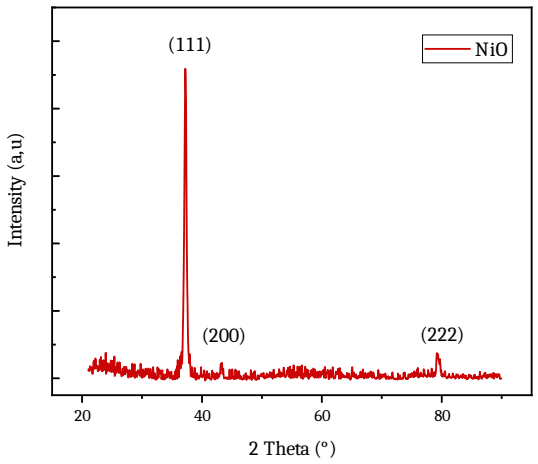

Figure 1. X-ray diffraction patterns of NiO film on the glass substrate.

The structural parameters of the sprayed thin film are listed in Table 2.

Table 2. Structural parameters of the elaborated sample.

Film	2θ (°)	d_{hkl} (Å)	a (Å)	D(nm)	ε (%)
NiO (111)	37,26	2,41	4,176	19,12	0,0018

The average size of the crystallite (D_{hkl}) corresponding to NiO is estimated from the XRD results using the Scherrer equation (Eq. (1)):

$$D_{hkl} = \frac{0{,}9\,\lambda}{\beta_{hkl}\,\cos\theta_{hkl}} \qquad (1)$$

Where θ_{hkl} corresponds to Bragg's diffraction angle, λ is the wavelength and β_{hkl} is the full width at Half-maximum intensity (FWHM) of the diffraction peak.

The lattice constant was determined using the cubic structure formula (Eq. (2)).

$$a = \frac{d_{hkl}}{\sqrt{h^2 + k^2 + l^2}} \qquad (2)$$

Where hkl are the Miller indices and d_{hkl} represents the inter-plenary distance.

The strain ε in the film can be estimated using the following equation (Eq. (3)).

$$\varepsilon = \frac{\beta_{hkl}\,\cos\theta_{hkl}}{4} \qquad (3)$$

4.2. Raman spectroscopy results

Figure 2 shows the Raman spectra of the NiO thin film in the range from 60 cm^{-1} to 1600 cm^{-1}. There are two prominent peaks around 550 cm^{-1} and 1100 cm^{-1}, suggesting the one-phonon first-order and two-phonon second-order longitudinal-optical modes respectively [29]. These results confirm that the nanocrystalline NiO is successfully deposited.

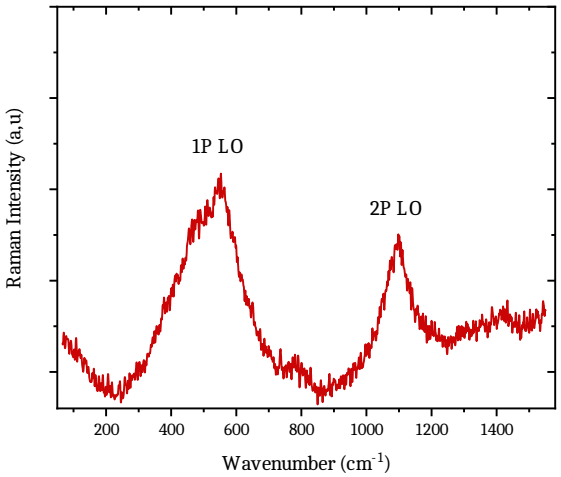

Figure 2. Raman spectra of NiO thin film.

4.3. Morphology

The surface morphology of the NiO layer was analyzed using The Scanning Electron Microscopy at different magnifications (7500 and 40.000 magnification). Figure 3 represents the morphological properties of the sprayed film on the glass substrate. The images of the NiO layer exhibit a smooth and dense surface suggesting a poor surface area of the film which is not helpful for a good electrochemical performance, However, the porous structure of the NiO layer provides a large reaction surface [30].

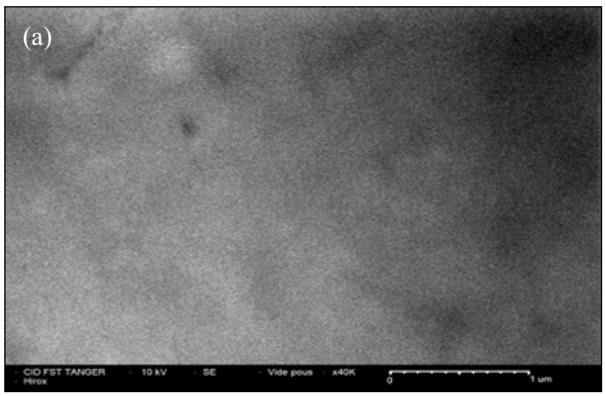

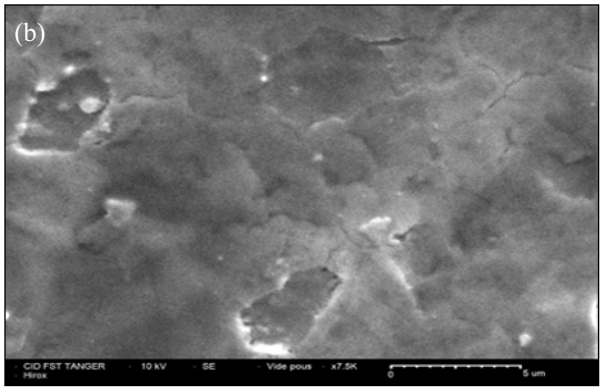

Figure 3. SEM images of the sprayed NiO film, (a) 40.000 magnification (b) 7500 magnification.

4.4. Optical properties

The measurement of optical spectrum for NiO thin film was carried out using a UV-VIS-NIR spectrometer. Figure 4 shows the transmission spectra of NiO thin film grown on the glass substrate in the 300–1500 nm wavelength range.

Figure.4 indicates that the transmittance is increased from low wavelength to higher wavelength region and the average transmission is about 55% in the visible light range. This relatively low value of the transmission may be due to the technique used.

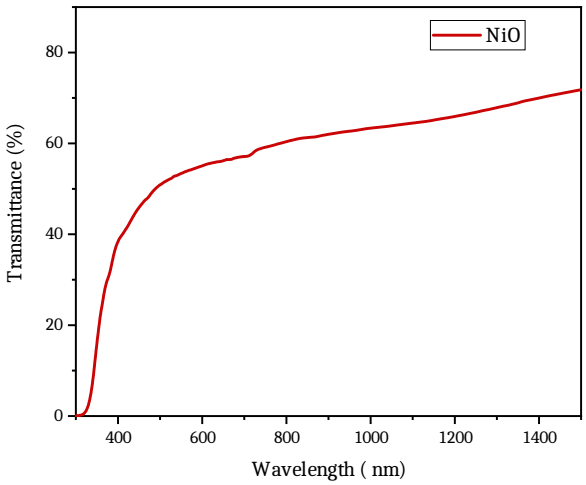

Figure 4. Transmittance spectra of NiO thin film.

The optical bandgap of the film was estimated using Tauc's equations:

$$(\alpha h\nu) = A\,(h\nu - Eg)^n \qquad (4)$$

Where, Eg the optical bandgap energy, A is a constant, and n = 2 for direct bandgap.

From the plots of $(\alpha h\upsilon)^2$ versus $h\upsilon$, Eg was calculated by extrapolating the linear portion of the curve to the energy axis for $(\alpha h\upsilon)^2 = 0$ (Figure 5).
The calculated energy bandgap value is 3,71 eV.

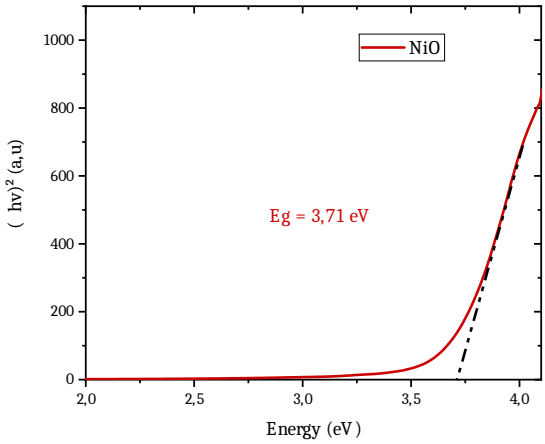

Figure 5. The $(\alpha h\nu)^2$ vs hν plots for NiO layer deposited on the glass substrate.

4.5. Electrochemical measurements

For the electrochemical study, a new sample is re-prepared with the same conditions cited in the experimental details section except for the glass substrate which is replaced by ITO substrate to ensure the conductivity of the elaborated NiO thin film (NiO/ITO).

The electrochemical properties of spray deposited NiO thin film are investigated in two different electrolytes such as 1M KOH and 1M NaOH by cyclic voltammetry. The measurement is investigated in the three-electrode system, consisting of NiO/ITO working electrode, Standard calomel electrode (SCE) reference electrode, and platinum (Pt) counter-electrode.

Figure 6 (a) and (b) show CV curves at different scan rates (5, 10, and 20 mv/s) of NiO thin film measured in the electrolytes cited previously.

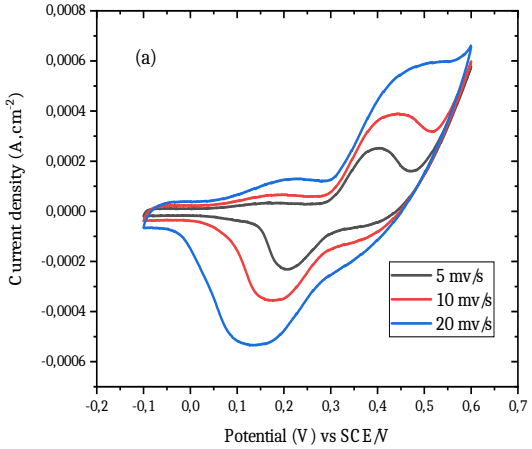

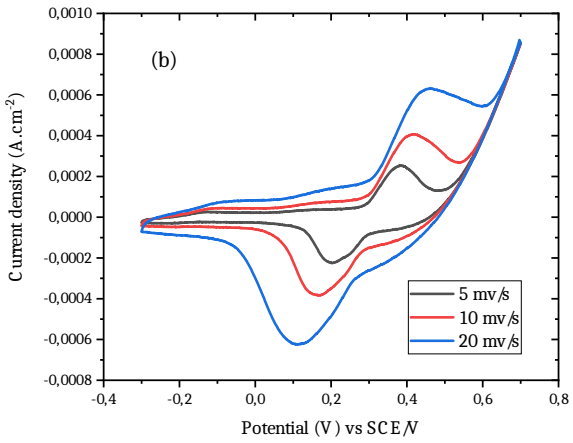

Figure 6. (a) CV curves of Pt/KOH 1M/SCE/NiO vs SCE (- 0.1V to 0.6V), (b) CV curves of Pt/NaOH 1M/SCE/NiO vs SCE (- 0.3V to 0.7V).

As observed, the shape of all (a) and (b) CV curves are almost the same with two redox peaks. Oxidation peak related to charging process and reduction peak for discharging process [31]. All CV peaks show that the current density increases with an increase in scan rate which proves the direct relationship between CV current and scan rate, suggesting an ideal capacitive characteristic [32]. Also, the small separation between redox peaks suggests a fast electron transfer behavior, which is very important for energy storage systems [31].

Specific capacitance 'Csp' is calculated from the relation [33]:

$$C_{sp} = \frac{1}{mv(V_c - V_a)} \int_{V_a}^{V_c} I(V)dV \qquad (5)$$

where, v is the potential scan rate ($mV.s^{-1}$), (Vc − Va) is a working potential window, (I) is the current response (mA) of the NiO electrode for the unit area (1 cm^2).

From Figure 7. it is observed that the value of specific capacitance decreases with an increase in scan rate for both electrolytes. This may be due to the fact that at a low scan rate there is sufficient time for transfer of charges between electrolyte and electrode interface. Maximum specific capacitance is found to be 24 $F.g^{-1}$ at a scan rate of 5 $mV.s^{-1}$ for KOH electrolyte.

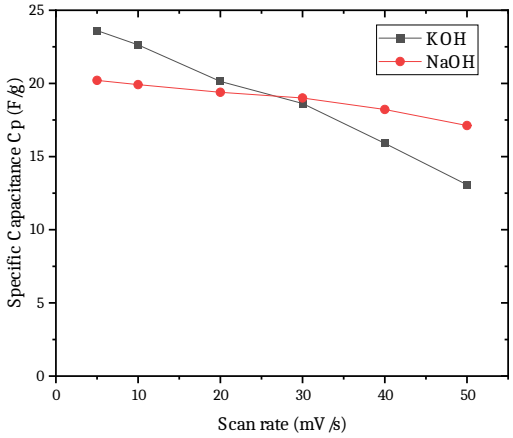

Figure 7. Variation of specific capacitance with scan rate in the KOH or NaOH electrolytes.

The general reaction or charge storage for nickel oxide electrode in the KOH or NaOH electrolytes is [34], [35]:

$$NiO + xOH^- \leftrightarrow xNiOOH + e^-$$

Where *x* represents K or Na metal elements.

The transition from NiO to NiOOH after intercalation of OH^- ions provoke charge transfer from Ni^{2+} to Ni^{3+}. Due to this transfer, the films get colored. During the cathodic scan, the reduction of Ni^{3+} to Ni^{2+}causes the bleaching of the film [36].

The transmittance spectra of the NiO layer in the colored and bleached states were recorded in the wavelength range of 350 to 850 nm, as shown in (Figure 8). The values are obtained after subtracting the transmittance of the ITO substrates using a UV-Vis-NIR spectrometer. This result is further used to calculate the coloration efficiency (CE) using the equation [14]:

$$CE_{\lambda=630nm} = \frac{(\Delta OD)_{630nm}}{Q_i} \qquad (6)$$

where (ΔOD) is the change in optical density at λ = 630 nm and Q_i is the intercalated charge (mC/cm^2).

The electrochromic parameters for the sample are given in Table 3. The value of CE is found to be a maximum of 15,15 cm^2/C for the electrolyte KOH. These calculated values are relatively low compared to the previous works, this may be due to the smooth morphology of the thin film, which does not allow good intercalation of OH^- ions [30].

Table 3. Electrochromic parameters of NiO film measured in alkaline solutions.

Electrolyte (1M)	ΔOD	Coloration efficiency (cm^2/C)
KOH	0,13	15,15
NaOH	0,076	7,8

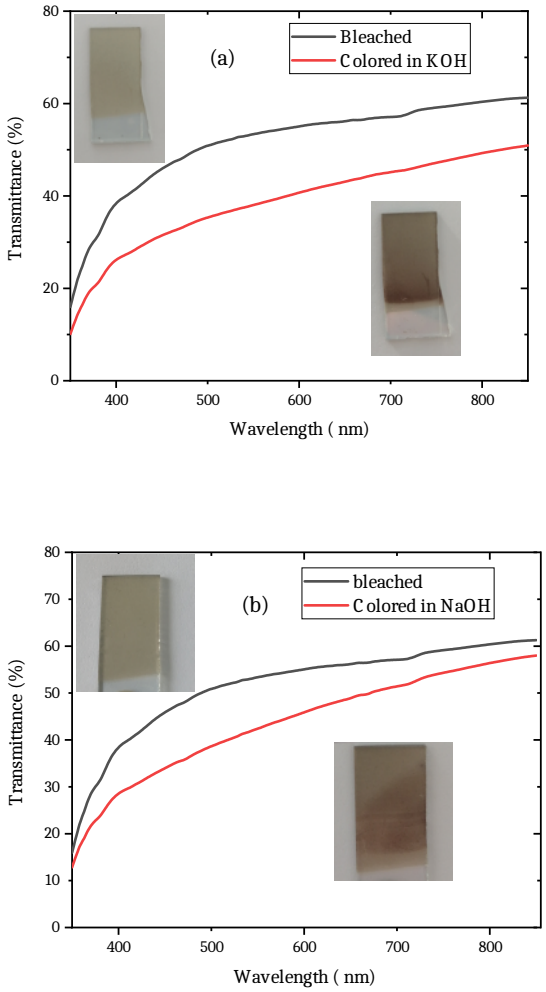

Figure 8. Optical transmittance in colored and bleached state of NiO thin layer recorded in: (a) 1 M KOH electrolyte at (-0,1 to 0,6 V vs SCE) (b) 1 M NaOH electrolyte at (-0,3 to 0,7 V vs SCE).

The stability of the film is one of the important parameters to be taken into account for electrochemical applications [37]. The CV stability of NiO film has been investigated by recording 50 cycles of the oxydo/reduction operation at a scan rate of 20 mV/s (Figure 9). From the stability measurements, it is observed that NiO film is stable in both electrolytes.

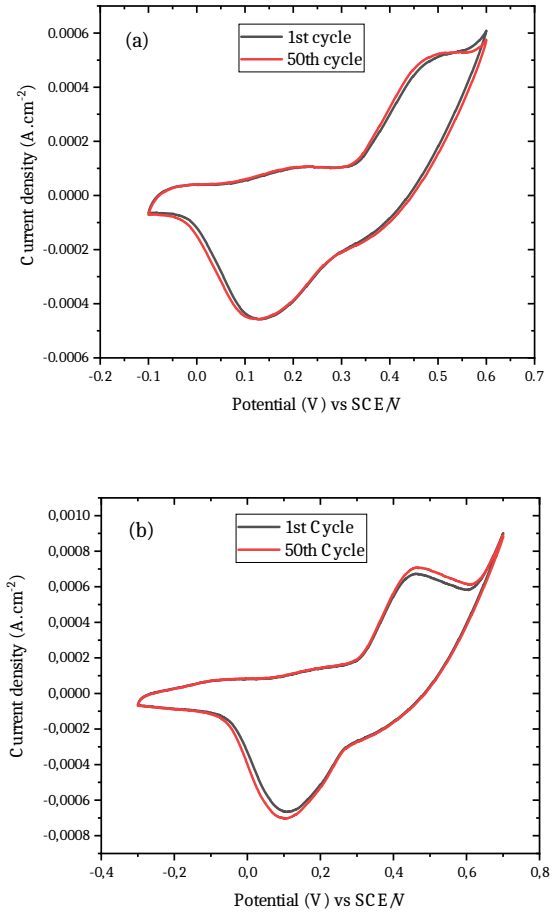

Figure 9. Cyclic voltammograms of NiO after 50th cycle at a scan rate of 20 mV/s in; (a) 1M KOH electrolyte (b) 1M NaOH electrolyte.

5. Conclusion

In this work, Nickel oxide thin film was successfully elaborated using the spray pyrolysis technique on the glass substrate. The structural, morphological, optical, and electrochemical properties were studied using X-ray diffraction, scanning electron microscope, UV–visible–NIR spectroscopy, and cyclic voltammetry techniques. The crystallographic study showed a polycrystalline cubic structure with preferential orientation on the plane (111). Surface morphology revealed a smooth and dense surface. Optical analysis showed an average transmission of about 55% in visible light range and gives an average direct band gap of 3,71 eV. Cyclic voltammograms of the sprayed film presented almost the same curves with two redox peaks. The Specific capacitance and the coloration efficiency of the NiO layer in 1M KOH were 24 Fg^{-1} (at the scan rate of 5 mv/s) and 15 cm^2/C respectively. These values decreased in 1M NaOH electrolyte to become 20 Fg^{-1} and 7,8 cm^2/C, which demonstrates the better performance of KOH than NaOH electrolyte. The stability measurement revealed that NiO film is stable in both electrolytes indicating its capability to insert/extract the ions for many cycles.

References

[1] R. O. Ijeh *et al.*, "Magnetic and optical properties of electrodeposited nanospherical copper doped nickel oxide thin films," *Physica E: Low-dimensional Systems and Nanostructures*, vol. **113**, pp. 233–239, Sep. 2019, doi: 10.1016/j.physe.2019.05.013.

[2] I. Fasaki, A. Koutoulaki, M. Kompitsas, and C. Charitidis, "Structural, electrical and mechanical properties of NiO thin films grown by pulsed laser deposition," *Applied Surface Science*, vol. **257**, no. 2, pp. 429–433, Nov. 2010, doi: 10.1016/j.apsusc.2010.07.006.

[3] H. Lee, Y.-T. Huang, M. W. Horn, and S.-P. Feng, "Engineered optical and electrical performance of rf–sputtered undoped nickel oxide thin films for inverted perovskite solar cells," *Sci Rep*, vol. **8**, no. 1, p. 5590, Apr. 2018, doi: 10.1038/s41598-018-23907-0.

[4] P. S. Patil and L. D. Kadam, "Preparation and characterization of spray pyrolyzed nickel oxide (NiO) thin films," *Applied Surface Science*, vol. **199**, no. 1, pp. 211–221, Oct. 2002, doi: 10.1016/S0169-4332(02)00839-5.

[5] Y. Akaltun and T. Çayır, "Fabrication and characterization of NiO thin films prepared by SILAR method," *Journal of Alloys and Compounds*, vol. **625**, pp. 144–148, Mar. 2015, doi: 10.1016/j.jallcom.2014.10.194.

[6] A. D. Jagadale, V. S. Kumbhar, D. S. Dhawale, and C. D. Lokhande, "Potentiodynamically deposited nickel oxide (NiO) nanoflakes for pseudocapacitors," *Journal of Electroanalytical Chemistry*, vol. **704**, pp. 90–95, Sep. 2013, doi: 10.1016/j.jelechem.2013.06.020.

[7] R. Paulose, R. Mohan, and V. Parihar, "Nanostructured nickel oxide and its electrochemical behaviour—A brief review," *Nano-Structures & Nano-Objects*, vol. **11**, pp. 102–111, Jul. 2017, doi: 10.1016/j.nanoso.2017.07.003.

[8] A. J. Haider, R. Al- Anbari, H. M. Sami, and M. J. Haider, "Photocatalytic Activity of Nickel Oxide," *Journal of Materials Research and Technology*, vol. **8**, no. 3, pp. 2802–2808, May 2019, doi: 10.1016/j.jmrt.2019.02.018.

[9] M. Tyagi, M. Tomar, and V. Gupta, "Optical Properties of NiO Thin Films: A Potential Material for Optoelectronic Devices," *Advanced Materials Research*, vol. **488–489**, pp. 103–108, 2012, doi: 10.4028/www.scientific.net/AMR.488-489.103.

[10] M. Napari *et al.*, "Antiferromagnetism and p-type conductivity of nonstoichiometric nickel oxide thin films," *InfoMat*, vol. **2**, no. 4, pp. 769–774, 2020, doi: 10.1002/inf2.12076.

[11] J. Jung, D. L. Kim, S. H. Oh, and H. J. Kim, "Stability enhancement of organic solar cells with solution-processed nickel oxide thin films as hole transport layers," *Solar Energy Materials and Solar Cells*,

vol. **102**, pp. 103–108, Jul. 2012, doi: 10.1016/j.solmat.2012.03.018.

[12] A. M. Soleimanpour, A. H. Jayatissa, and G. Sumanasekera, "Surface and gas sensing properties of nanocrystalline nickel oxide thin films," *Applied Surface Science*, vol. **276**, pp. 291–297, Jul. 2013, doi: 10.1016/j.apsusc.2013.03.085.

[13] G. S. Gund, C. D. Lokhande, and H. S. Park, "Controlled synthesis of hierarchical nanoflake structure of NiO thin film for supercapacitor application," *Journal of Alloys and Compounds*, vol. **741**, pp. 549–556, Apr. 2018, doi: 10.1016/j.jallcom.2018.01.166.

[14] H. Lin *et al.*, "The growth, properties and application of reactively sputtered nickel oxide thin films in all thin film electrochromic devices," *Materials Science and Engineering: B*, vol. **270**, p. 115196, Aug. 2021, doi: 10.1016/j.mseb.2021.115196.

[15] S. J. Lee, T.-G. Lee, S. Nahm, D. H. Kim, D. J. Yang, and S. H. Han, "Investigation of all-solid-state electrochromic devices with durability enhanced tungsten-doped nickel oxide as a counter electrode," *Journal of Alloys and Compounds*, vol. **815**, p. 152399, Jan. 2020, doi: 10.1016/j.jallcom.2019.152399.

[16] H. Yang, J.-H. Yu, H. J. Seo, R. H. Jeong, and J.-H. Boo, "Improved electrochromic properties of nanoporous NiO film by NiO flake with thickness controlled by aluminum," *Applied Surface Science*, vol. **461**, pp. 88–92, Dec. 2018, doi: 10.1016/j.apsusc.2018.05.231.

[17] A. S. Kondrateva, M. V. Mishin, and S. E. Alexandrov, "TOF MS Investigation of Nickel Oxide CVD," *J. Am. Soc. Mass Spectrom.*, vol. **28**, no. 11, pp. 2352–2360, Nov. 2017, doi: 10.1007/s13361-017-1765-1.

[18] M. H. Raza *et al.*, "Tuning the NiO Thin Film Morphology on Carbon Nanotubes by Atomic Layer Deposition for Enzyme-Free Glucose Sensing," *ChemElectroChem*, vol. 6, no. **2**, pp. 383–392, 2019, doi: 10.1002/celc.201801420.

[19] P. Salunkhe, M. A. A.V, and D. Kekuda, "Structural, spectroscopic and electrical properties of dc magnetron sputtered NiO thin films and an insight into different defect states," *Appl. Phys. A*, vol. **127**, no. 5, p. 390, Apr. 2021, doi: 10.1007/s00339-021-04501-0.

[20] M. A. Hameed, O. A. Ali, and S. S. M. Al-Awadi, "Optical properties of Ag-doped nickel oxide thin films prepared by pulsed-laser deposition technique," *Optik*, vol. **206**, p. 164352, Mar. 2020, doi: 10.1016/j.ijleo.2020.164352.

[21] D. R. Sahu, T.-J. Wu, S.-C. Wang, and J.-L. Huang, "Electrochromic behavior of NiO film prepared by e-beam evaporation," *Journal of Science: Advanced Materials and Devices*, vol. **2**, no. 2, pp. 225–232, Jun. 2017, doi: 10.1016/j.jsamd.2017.05.001.

[22] K. O. Ukoba, A. C. Eloka-Eboka, and F. L. Inambao, "Review of nanostructured NiO thin film deposition using the spray pyrolysis technique," *Renewable and Sustainable Energy Reviews*, vol. **82**, pp. 2900–2915, Feb. 2018, doi: 10.1016/j.rser.2017.10.041.

[23] S. Zargouni, S. El Whibi, E. Tessarolo, M. Rigon, A. Martucci, and H. Ezzaouia, "Structural properties and defect related luminescence of Yb-doped NiO sol-gel thin films," *Superlattices and Microstructures*, vol. **138**, p. 106361, Feb. 2020, doi: 10.1016/j.spmi.2019.106361.

[24] J.-H. Yu, S.-H. Nam, Y. E. Gil, and J.-H. Boo, "The effect of ammonia concentration on the microstructure and electrochemical properties of NiO nanoflakes array prepared by chemical bath deposition," *Applied Surface Science*, vol. **532**, p. 147441, Dec. 2020, doi: 10.1016/j.apsusc.2020.147441.

[25] B. R. Cruz-Ortiz, M. A. Garcia-Lobato, E. R. Larios-Durán, E. M. Múzquiz-Ramos, and J. C. Ballesteros-Pacheco, "Potentiostatic electrodeposition of nanostructured NiO thin films for their application as electrocatalyst," *Journal of Electroanalytical Chemistry*, vol. **772**, pp. 38–45, Jul. 2016, doi: 10.1016/j.jelechem.2016.04.020.

[26] H. Ftouhi, Z. E. Jouad, M. Jbilou, M. Diani, and M. Addou, 'Study of microstructural, morphological and optical properties of sprayed vanadium doped ZnO nanoparticles', *Eur. Phys. J. Appl. Phys.*, vol. **87**, no. 1, Art. no. 1, Jul. 2019, doi: 10.1051/epjap/2019190111.

[27] P. S. Patil and L. D. Kadam, "Preparation and characterization of spray pyrolyzed nickel oxide (NiO) thin films," *Applied Surface Science*, vol. **199**, no. 1, pp. 211–221, Oct. 2002, doi: 10.1016/S0169-4332(02)00839-5.

[28] S. A. Hameed, M. M. Kareem, Z. T. Khodair, and I. M. Mohammed Saeed, "The influence of deposition temperatures on the structural and optical properties for NiO nanostructured thin films prepared via spray pyrolysis technique," *Chemical Data Collections*, vol. **33**, p. 100677, Jun. 2021, doi: 10.1016/j.cdc.2021.100677.

[29] K. S. Usha, R. Sivakumar, C. Sanjeeviraja, V. Sathe, V. Ganesan, and T. Y. Wang, "Improved electrochromic performance of a radio frequency magnetron sputtered NiO thin film with high optical switching speed," *RSC Adv.*, vol. **6**, no. 83, pp. 79668–79680, Aug. 2016, doi: 10.1039/C5RA27099E.

[30] X. H. Xia, J. P. Tu, J. Zhang, X. L. Wang, and W. K. Zhang, "Morphology effect on the electrochromic and electrochemical performances of NiO thin films," *Electrochimica Acta*, vol. **53**, no. 18, pp. 5721–5724, Jul. 2008, doi: 10.1016/j.electacta.2008.03.047.

[31] A. A. Yadav and U. J. Chavan, "Influence of substrate temperature on electrochemical supercapacitive performance of spray deposited nickel oxide thin films," *Journal of Electroanalytical Chemistry*, vol. **782**, pp. 36–42, Dec. 2016, doi: 10.1016/j.jelechem.2016.10.006.

[32] C.-C. Hu and T.-W. Tsou, "Ideal capacitive behavior of hydrous manganese oxide prepared by anodic deposition," *Electrochemistry Communications*, vol. **4**, no. 2, pp. 105–109, Feb. 2002, doi: 10.1016/S1388-2481(01)00285-5.

[33] A. A. Yadav, "SnO2 thin film electrodes deposited by spray pyrolysis for electrochemical supercapacitor applications," *Journal of Materials Science: Materials in Electronics*, vol. **27**, no. 2, pp. 1866–1872, 2016, doi: 10.1007/s10854-015-3965-4.

[34] S. Vijayakumar, S. Nagamuthu, and G. Muralidharan, "Supercapacitor studies on NiO nanoflakes synthesized through a microwave route," *ACS Applied Materials and Interfaces*, vol. **5**, no. 6, pp. 2188–2196, 2013, doi: 10.1021/am400012h.

[35] J. Zhao, Y. Tian, A. Liu, L. Song, and Z. Zhao, "The NiO electrode materials in electrochemical capacitor: A review," *Materials Science in Semiconductor Processing*, vol. **96**, pp. 78–90, Jun. 2019, doi: 10.1016/j.mssp.2019.02.024.

[36] D. Dong *et al.*, "Electrochromic properties of NiOx:H films deposited by DC magnetron sputtering for ITO/NiOx:H/ZrO2/WO3/ITO device," *Applied Surface Science*, vol. **357**, pp. 799–805, Dec. 2015, doi: 10.1016/j.apsusc.2015.09.056.

[37] Z. Li *et al.*, "Nickel oxide film with tertiary hierarchical porous structure and high electrochromic performance and stability," *Materials Chemistry and Physics*, vol. **269**, p. 124738, Sep. 2021, doi: 10.1016/j.matchemphys.2021.124738.